Journal of Thermal Analysis and Calorimetry, Vol. 79 (2005) 107–113

THE THERMAL DECOMPOSITION BEHAVIOR OF RDX-BASE PROPELLANTS

W.-W. Jing[1], *Z.-M. Dang*[2*] *and G.-P. Yang*[1]

[1]Department of Chemistry and Chemical Industry, Ocean University of China, Qingdao 266003, P.R. China
[2]College of Material Science and Engineering, Beijing University of Chemical Technology, Beijing 100029, P.R. China

In this paper, the thermal decomposition of cyclotrimethylenetri-nitramine (RDX)-base propellants involving many components has been investigated by differential scanning calorimeter (DSC). The decomposition characters at different heating rates and the activation energies are determined by DSC measurement. The results show that the decomposition of RDX is accelerated obviously during the decomposition of nitroglycerin (NG). Though the content of dibutyl-benzene-dicarbonate (DBP) ingredient in the propellants is less, it has a remarkable effect on the initial decomposition temperature of the propellants. The azido-nitromine compound (DIANP) brings about the shift of the peak of decomposition of RDX and nitrocellulose (NC) to lower temperature due to its liquefying or dissolving.

Keywords: *cyclotrimethylenetri-nitramine (RDX)-base propellants, DSC, thermal decomposition behavior*

Introduction

Nitramine propellants (NAPs) with high energy and low combustion corrosion have become a prospective new gun propellants. Therefore, new development of NAPs has been paid much attention in the world [1–3]. However, NAPs commonly exist several combustion pressure indexes and might cause a damage of the ballistic efficiency and the reproducibility of the ballistic performance. This is one of main troubles for their wide application. It is very important to study on the initial thermal decomposition of these kinds of NAPs. Hitherto, there are few research found in the literature [4], and several approaches have been undergone in order to find out the relationship between the thermal decomposition behavior and combustion properties [1].

Thus, the research in this study focuses on the thermal decomposition behaviors of NAPs. Here we design the different component NAPs and investigate their thermal decomposition behavior by DSC, and also attempt to find an interacting relationship between the thermal decomposition behavior and component of NAPs and thereby contribute a thorough research of thermal decomposition and combustion character.

Experimental

Samples

The components of the NAPs used in this work are listed in Table 1.

Differential scanning calorimetry

A PerkinElmer DSC-2C instrument was employed in this work. All tests were carried out with a nitrogen flow rate 40 cm^3 min^{-1} and at heating rates of 5, 10, 20 and 40°C min^{-1} respectively. The amount of NAPs samples was about 2 mg and they were put into aluminum crucible, respectively.

Results and discussions

The character of DSC curve

Figure 1a, b is DSC curve of NAPs with NG and DIANP respectively, at heating rate 10°C min^{-1}. It is shown from Fig. 1 that sample 1 and 11 (without RDX) possess only one decomposition exothermic peak at about 200°C, while other samples with RDX have two peaks. Compared these curves with pure RDX curve and with thermal decomposition behaviors of other components, it is assumed that the first peak is caused by decomposition of NC and NG or NC and DIANP and second one by RDX. The whole thermal decomposition involves the decomposition of NC and NG or NC and DIANP double-base binders and RDX. Thermal decomposition occurs in two steps and each step is individual.

In addition, from the DSC curves of sample 1 at different heating rates 5, 10, 20 and 40°C min^{-1} respectively (Fig. 2), it is noticed that the composition peaks are divided into two single peaks with an increase in heating rate. This result is clearly shown that

---

[*] Author for correspondence: dangzm@mail. buct.edu.cn

1388–6150/$20.00

Akadémiai Kiadó, Budapest, Hungary
Springer, Dordrecht, The Netherlands

Table 1 The formulations of the NAPs

Sample No.	*w*(NC)/ %	*w*(NG)/ %	*w*(DIANP)/ %	*w*(DBP) %	*w*(RDX)/ %	RDX size μm
1	65.00	28.00	0	5.00	0	20
2	26.00	11.20	0	2.00	60	20
3	35.75	15.40	0	2.75	45	20
4	45.50	19.60	0	3.50	30	20
5	55.25	23.80	0	4.25	15	20
6	55.25	26.62	0	1.42	15	20
7	45.50	19.60	0	3.50	30	100
8	45.50	19.60	0	3.50	30	50
9	45.50	19.60	0	3.50	30	10
10	45.50	19.60	0	3.50	30	3~5
11	65.00	0	33.00	0	0	20
12	26.00	0	13.20	0	60	20
13	35.75	0	18.15	0	45	20
14	45.50	0	23.10	0	30	20
15	55.25	0	28.05	0	15	20
16	55.25	14.23	13.82	0	15	20

the two peaks possess different temperature shift with increasing the heating rate and different activation energy. NC possesses higher activation energy of decomposition than NG does. According to the results, it is determined the first peak is attributed to NG decomposition and the second one is to NC. The data of various heating rates are listed in Table 2.

Based on Kissinger's equation [5, 6]:

$$\ln(\beta/T_m^2)=\ln(AR/E)–E/RT_m$$

here T_m is the melting peak temperature and β is the heating rates. The kinetic parameters of thermal decomposition can be found by a least-squares regression. The results are listed in Table 3 including activation energy *E* and ex-exponential factor *A*.

Table 2 Decomposition peak temperature on DSC at various heating rates (β/°C min^{-1})

Sample No.	β=5		β=10		β=20		β=40	
	T_{m1}/°C	T_{m2}/°C	T_{m1}/°C	T_{m2}/°C	T_{m1}/°C	T_{m2}/°C	T_{m1}/°C	T_{m2}/°C
1	193.2	229.2	200.6	203.0	206.8	210.5	213.8	217.9
2	199.8	229.2	205.9	240.3	214.2	250.1	223.9	261.1
3	196.3	226.6	204.6	237.9	213.5	247.5	223.1	258.2
4	194.8	228.6	203.6	239.0	201.9	248.0	221.3	258.3
5	194.0	231.2	202.9	234.6	211.3	249.6	220.6	257.6
6	196.0	231.8	204.1	234.0	211.4	248.6	220.5	257.8
7	194.9	229.1	204.6	237.7	211.0	247.5	221.5	258.0
8	195.0	228.6	204.6	237.6	212.2	248.3	221.1	257.8
9	195.2	228.8	204.5	238.5	212.0	248.3	221.5	258.0
10	193.5	228.6	201.9	237.5	210.1	247.5	219.2	258.0
11	193.2	–	200.5	–	209.1	–	219.0	–
12	193.8	222.0	202.2	233.6	210.3	243.2	219.9	253.2
13	193.3	219.5	200.9	229.2	208.9	239.2	219.1	250.3
14	193.2	219.3	200.6	228.8	208.5	238.8	217.2	249.3
15	192.2	217.9	200.3	227.5	207.5	238.5	216.3	247.7
16	190.9	219.0	200.4	226.6	207.3	238.5	215.9	248.4

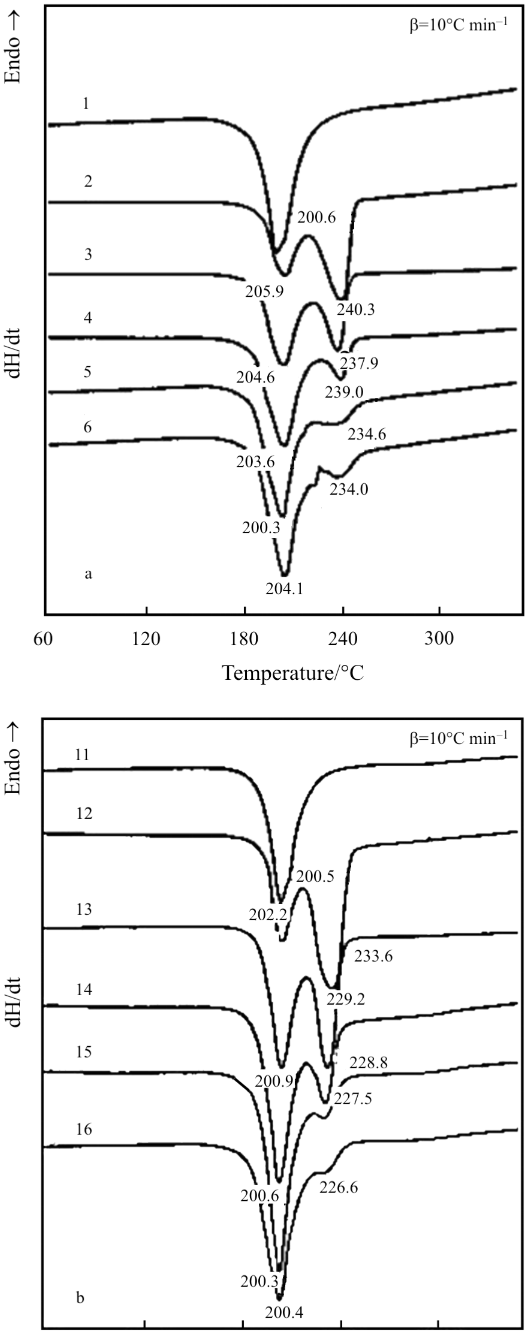

Fig. 1 DSC curves of a – samples 1–6 and b – samples 11–16

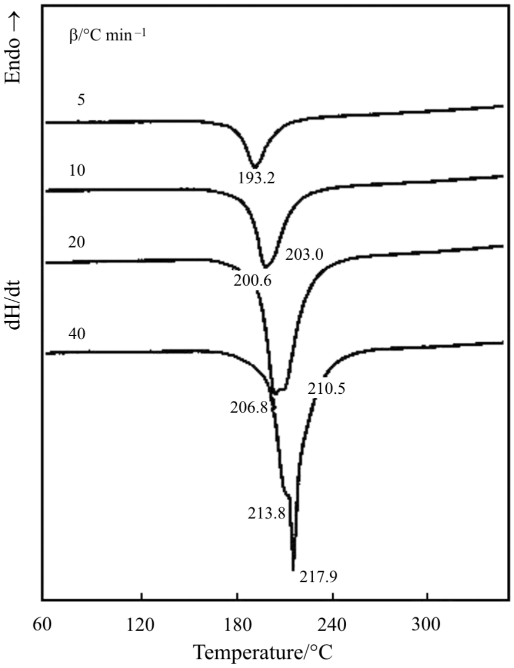

Fig. 2 DSC curves of sample 1 at different heating rates

Effect of RDX on the thermal decomposition of NAPs

From T_{m1} and E_1 data in Table 3, it is found that the E_1 of sample 1 without RDX is about 184.3 kJ mol^{-1}, while the E_1 of sample 2 with 60% RDX is down to 158.7 kJ mol^{-1}. The result shows that RDX partially has an effect on the first decomposition reaction. A comparison of the E_1 of sample 11 without RDX with that of sample 12 with 60% RDX, it gives almost the same value, 145.4 kJ mol^{-1} and 145.5 kJ mol^{-1}. The only difference of samples 1 and 2 from samples 11 and 12 is the former components containing NG+DBP and the later containing DIANP. It is suggested that RDX has an important effect on NG decomposition and no clear effect on NC decomposition.

From DSC curves of NC, RDX and NC/RDX in Fig. 3, the decomposition peak of RDX is slightly changed from 208.6 to 208.0°C when it mixes with NC. It is a further confirmation to referring results above.

It is worthwhile to note that, as shown in Table 3, there is no relationship between E_1 and the amount of RDX. Though RDX content is reduced from 60% in sample 2 to 15% in sample 6, E_1 value of samples 2 and 6 is about 158.7 kJ mol^{-1} and samples 3 to 5 have lower E_1. This is clearly shown that RDX has an effect on NG decomposition, but does not on the activation energy.

Effect of DBP on the thermal decomposition of NAPs

It is seen, from T_{m1} values of samples 1 to 5 at various heating rates in Table 2, T_{m1} is down with an increase in DBP content (Fig. 4a). A further investigation on NC, NC/NG and (NC+NG)/DBP shows that the peak temperature of decomposition of NC with 30% NG is slightly changed from 208.6 to 207.9°C and it is dramatically changed (from 208.6 to 202.9°C) when a

Table 3 Kinetic parameters of thermal decomposition of NAPs samples

Sample No.	E/kJ mol^{-1}		lg$A$/s^{-1}		r^*	
	T_{m1}/°C	T_{m2}/°C	T_{m1}/°C	T_{m2}/°C	T_{m1}/°C	T_{m2}/°C
1	184.3	–	22.1	–	0.9991	–
2	158.7	137.9	19.0	15.6	0.9959	0.9994
3	142.3	137.8	17.2	15.7	0.9998	0.9990
4	143.8	149.0	17.4	16.8	0.9998	0.9995
5	142.7	147.2	17.3	16.6	0.9998	0.9730
6	157.0	147.8	18.9	16.7	0.9994	0.9657
7	145.7	150.6	17.6	17.0	0.9959	0.9995
8	148.2	147.5	17.9	16.7	0.9998	0.9995
9	146.2	146.5	17.7	16.6	0.9988	0.9999
10	147.2	147.7	17.9	16.7	0.9999	0.9997
11	145.4	–	–	–	–	–
12	145.5	136.6	17.7	15.7	0.9996	0.9981
13	146.4	136.7	17.8	15.8	0.9983	0.9999
14	156.9	139.8	19.0	16.2	0.9997	0.9999
15	157.0	138.2	19.0	16.0	0.9995	0.9991
16	151.1	138.4	8.4	16.0	0.9975	0.9970

$^*r$–regression correlation coefficient

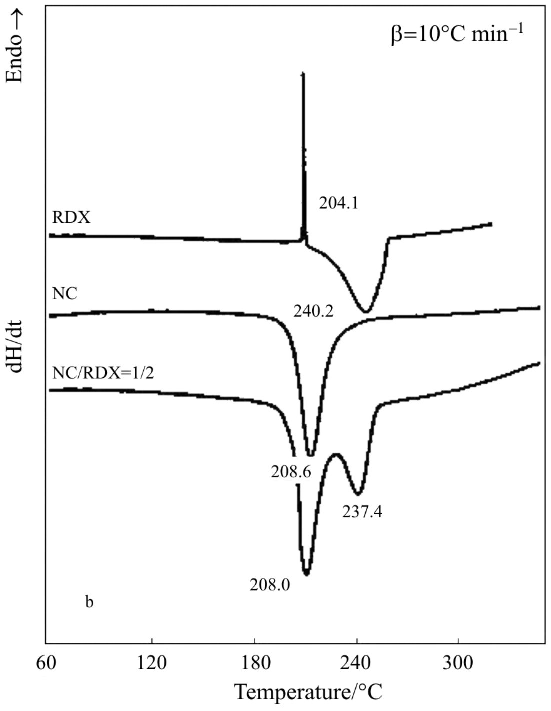

Fig. 3 DSC curves of NC, RDX and NC/RDX mixed system

small amount of DBP is used (Fig. 4b). When we carefully compare the T_{m2} data of samples 2–6 in Table 2, there are irregular changes occurred, which means that RDX decomposition is not interfered at a small amount DBP existence.

Effect of DIANP on the thermal decomposition of NAPs

Samples 2 and 12, 3 and 13, 4 and 14, 5 and 15 are chosen in this study, in which each couple contains the same content of NC and RDX, but one contains NG and another does DIANP, in order to studying the effect of DIANP on decomposition of NAPs. The difference of ΔT_m between T_{m1} and T_{m2} of the couples at various heating rates are given in Table 4.

All of the data in Table 4 show that the decomposition temperature of NAPs is obviously decreased when DIANP replaces NG. Unlike NG, DIANP accelerates not only decomposition of NC, but also decomposition of RDX. A decrease in ΔT_{m2} is much more than that in ΔT_{m1}, which indicates that DIANP has stronger effect on the decomposition of RDX than that of NC. In general, there is a difference between the values of ΔT_{m1} or ΔT_{m2} at different heating rates. However, the more DIANP contents in NAPs sample cause a greater ΔT_{m2}, as showing in Table 4.

In addition, ΔT_{m1} and ΔT_{m2} are down with increasing DIANP (Fig. 5). T_{m2} is down more obvious than T_{m1}. A comparison of ΔT_{m1} and ΔT_{m2} from sample couples 6 and 16 with 5 and 15 shows that the almost same results as referring above arises after DIANP is instead of NG. Further confirmation is obtained by a comparison of T_{m1} and T_{m2} from samples

Table 4 ΔT_{m1} and ΔT_{m2} valuesof the sample couples at various heating rates

Sample couple	DIANP/ %	ΔT_{m1}				ΔT_{m2}			
		β/°C min^{-1}							
		5	10	20	40	5	10	20	40
2–12	13.2	6.0	3.7	3.9	4.0	7.2	6.7	6.9	7.9
3–13	18.15	3.0	3.7	4.6	4.0	7.1	8.7	8.3	7.9
4–14	23.10	1.6	3.0	3.4	4.1	9.5	10.2	9.2	9.0
5–15	28.05	1.8	2.6	3.8	4.3	13.3	7.1	11.1	9.9
6–16	13.82	5.1	3.7	4.1	4.6	12.8	7.4	10.1	9.4

16 and 15. In a view of activation energy data, although the decomposition of NC and RDX is accelerated by DIANP, there are no obvious effect of DIANP on activation energy of NC and RDX, which indicates that decomposition mechanisms of NC and RDX do not change with a replacement of NG with DIANP.

DIANP, a liquid, may dissolve RDX and NG and the amount of dissolvent increase with rising temperature. According to experimental results, at temperature 180°C, RDX and DIANP dissolve each other to form a homogeneous liquid. As it is well known that a substance in liquid is decomposed faster than that in solid. Under DSC measurement condition, NC and RDX decompose at temperature above 190°C, which suggests that RDX decompose in liquid phase and NC decomposes in partially liquid phase. The decomposi-

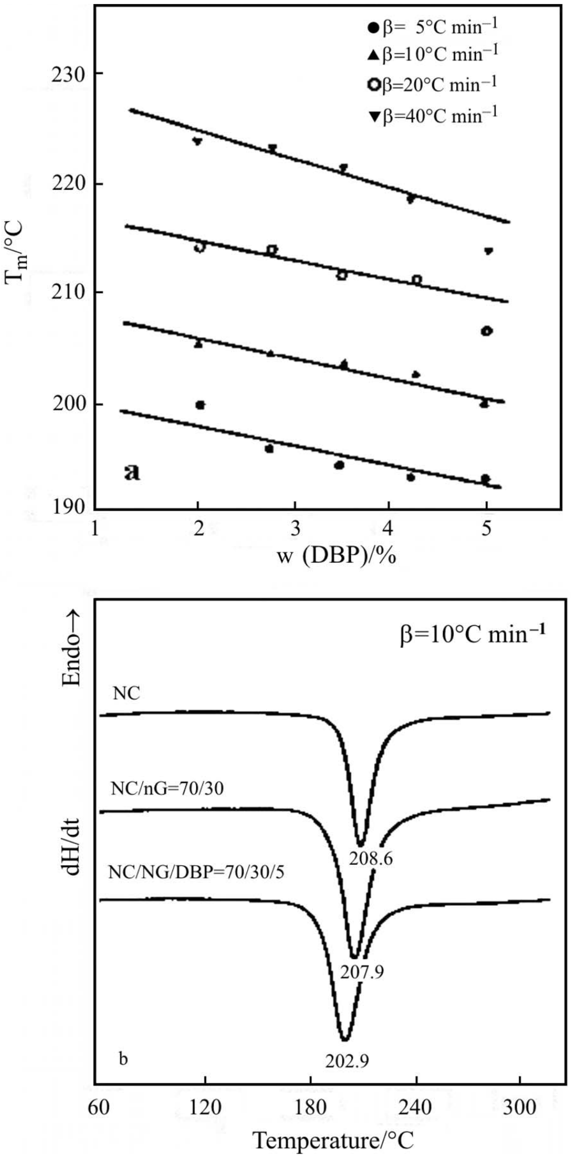

Fig. 4 a – The dependence of T_m on *w* (DBP)% and b – DSC curves of NC, NC/NG and NC/NG/DIANP mixed system

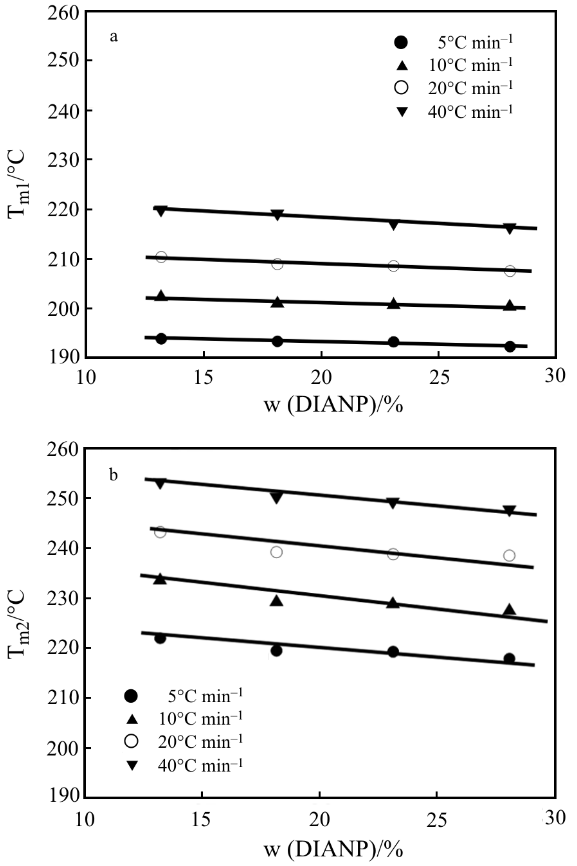

Fig. 5 a – The dependence of T_{m1} on *w* (DIANP) % and b – the dependence of T_{m2} on *w* (DIANP)%

tion temperature decreases with increasing DIANP, therefore, T_{m2} and ΔT_{m2} is also decreased with an increase of DIANP.

In Fig. 6, by comparison of DSC curves of NC, RDX, NC/DIANP and RDX/DIANP, it is found that the decomposition peak temperatures of NC and RDX on DSC decrease from 208.6 and 240.4°C to 202.3 and 236.8°C, respectively. In RDX/DIANP mixed system, the melting peak of RDX disappears on DSC curve, which indicates that RDX is melt or dissolved by DIANP before its decomposition and thereby the initial decomposition temperature T_0 of RDX is decreased from 218.5 to 209.8°C. All of these results further prove to have a prompting action of DIANP on the decomposition of NC and RDX.

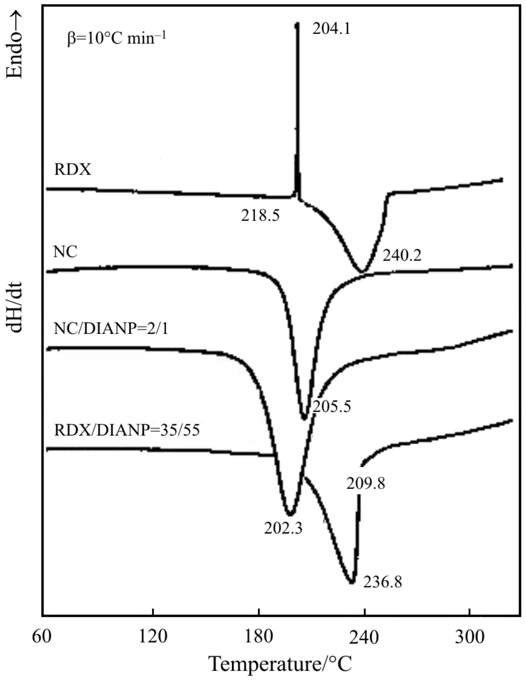

Fig. 6 DSC curves of NC, RDX, NC/DIANP and RDX/DIANP

Effect of RDX particle size on the thermal decomposition of NAPs

The components of sample 7–10 in Table 1 are the same but the particle size of RDX is different, which all decomposition temperature is almost unchanged when RDX particle size over 10 μm, even under different heating rates, and the decomposition temperature T_{m1} is decreased intensively when RDX particle size is about 3–5 μm. Clearly enough, the effect of particle size on decomposition occurred only at solid-state surface reaction condition. From this result, it is proposed that the decomposition reaction rate increase and T_{m1} decrease when RDX is used in small particle size with large surface area. T_{m2} does not change with different particle size because T_{m2} peak is the decomposition of residue after first decomposition. Furthermore, the data in Table 3 are also provided evidence that the particle size of RDX does not change activation energy, namely, no any change of decomposition mechanism in this kind of NAPs.

Conclusions

- The decomposition of RDX is accelerated obviously during the decomposition of NG.
- Though the content of DBP ingredient in the propellants is less, it has a remarkable effect on the initial decomposition temperature of the propellants.
- The DIANP brings about the shift of the peak of decomposition of RDX and NC to lower temperature due to its liquefying or dissolving.
- The particle size of RDX when larger than 10 μm has a negligible effect on the decomposition of NAPs.

Appendix

DSC	Differential scanning calorimeter
RDX	Cyclotrimethylenetri–nitramine
NC	Nitrocellulose
DIANP	Azido-nitromine compound
DBP	Dibutyl-benzene-dicarbonate
NG	Nitroglycerine
NAPs	Nitramine propellants
T_{m1}	First decomposition exothermic peak temperature
T_{m2}	Second decomposition exothermic peak temperature
ΔT_{m1}	Difference in temperature between T_{m1}
ΔT_{m2}	Difference in temperature between T_{m2}
β	Heating rate
E	Activation energy
A	Pre-exponential factor
R	Thermal dynamics constant
r	Regression correlation coefficient
E_1	Activation energy corresponding to T_{m1}
T_0	Initial decomposition temperature

Acknowledgements

We thank especially Mr. Shu-Jun Jiang, Zi-Ru Liu and Cheng-Zhong Du for their great help.

References

1 S. W. Li, J. Propulsion Technology, 4 (1995) 61 (in Chinese).
2 E. Kimura and Y. Oyumi, Propellant, Explosive, Pyrotechnics, 20 (1995) 322.

3 Z. Dang and F. Zhao, J. Therm. Anal. Cal., 61 (2000) 771.
4 Y. Oyumi and K. Inokami, Propellants, Explosives, Pyrotechnics, 19 (1995) 180.
5 A. Mianowski, J. Therm. Anal. Cal., 74 (2003) 953.
6 A. Mianowski and R. Bigda, J. Therm. Anal. Cal., 75 (2004) 335.

Received: March 4, 2004
In revised form: April 14, 2004